

Shell Biosciences Laboratory, Sittingbourne, Kent, U. K.

# Light and electron microscopical studies of the infection of *Vitis* spp. by *Plasmopara viticola*, the downy mildew pathogen

by

P. LANGCAKE and PATRICIA A. LOVELL

## Licht- und elektronenmikroskopische Untersuchungen über die Infektion von *Vitis* spp. durch *Plasmopara viticola*, den Erreger des Falschen Rebenmehltaus

**Zusammenfassung.** — Die Infektion der anfälligen Europäerrebe (*Vitis vinifera* L.) und einer resistenten Wildart (*V. riparia* MICHX.) durch den Erreger des Falschen Mehltaus (*Plasmopara viticola*) wurde mittels Licht- und Elektronenmikroskopie untersucht. Der Infektionsablauf und die ultrastrukturellen Besonderheiten der Krankheit werden eingehend beschrieben und mit dem Erscheinungsbild anderer Wirt-Parasit-Beziehungen verglichen.

### Introduction

*Plasmopara viticola* (B. et C.) BERL. et DE TONI, the grapevine downy mildew pathogen, causes economically a very important disease. The fungus has a narrow host range, being parasite on *Vitis vinifera* (the cultivated grapevine) and a few other *Vitis* species. Although some limited development of the fungus may occur in certain other members of the family Vitaceae, all plants outside this family are highly resistant or immune (4). Despite their economic importance, the downy mildews in general have received very little attention particularly from the biochemical but also from the histological point of view and this is particularly true of *P. viticola*. Comparatively detailed light and electron microscopical studies of the downy mildew disease of lettuce (caused by *Bremia lactucae*) have been carried out (13, 27). Other downy mildews which have been studied are those of hop (21, 22), cucumber (15), cabbage (7) and soybean (23). In addition, there are several structural studies of the related late blight disease caused by *Phytophthora infestans* (8, 28, 29).

The present study was undertaken to provide a morphological background to the current biochemical studies on the reaction of grapevine to downy mildew (17) in view of the paucity of information on *P. viticola* in the literature (although some studies have been reported (1, 9, 10, 18)). Some observations on the reaction of *V. riparia*, which is resistant to *P. viticola*, are also made.

### Methods

Young, fully expanded leaves of plants of *V. vinifera* (var. Carbernet Sauvignon) and *V. riparia* (var. Gloire de Montpellier) were inoculated by spraying the under-

surfaces of the leaves with a dense (ca  $5 \times 10^4$ /ml) suspension of sporangia of *P. viticola*. The plants were incubated at ca. 23 °C in continuous 100 % R. H. in the greenhouse. Under these conditions, dense and uniform infections of the leaves were obtained and, in *V. vinifera*, sporulation occurred approximately 96 h after inoculation.

For the examination of cleared leaf segments, samples of infected tissue (14 mm diam. discs) were cut from the leaves and stained either according to a modified acid fuchsin method of GALBIATI (10) in which the initial clearing of the leaves was carried out at 60 °C for 1 h rather than 7 d at room temperature, or to the trypan blue method used by JONES and DEVERALL (14). Segments were mounted on glass slides in 50 % glycerol and examined directly under the light microscope.

For examination of leaf sections of *V. vinifera* by light and transmission electron microscopy, samples (1 mm  $\times$  5 mm) of infected leaf were fixed under vacuum for 2 h in 4 % glutaraldehyde in 0.1 M SØRENSEN phosphate buffer (pH 7.4) containing Tween 20 (2 drops in 5 ml). Samples were washed overnight in the phosphate buffer containing 10 % sucrose, then post-fixed for 2 h under vacuum in 1 % OsO<sub>4</sub> in the phosphate buffer and washed three times in the buffer. They were dehydrated through an ethanol series (30, 50, 70 and 90 %, 10 min in each), then in changes of absolute ethanol for 10, 20 and 30 min, respectively. Tissues were then infiltrated under vacuum for 2 h each in ethanol : SPURR resin (33) mixtures of 1 : 1 and 1 : 3, then in SPURR resin overnight. The resin was changed, then polymerised at 70 °C for 48 h.

Sections were cut using glass knives on an LKB Ultratome III instrument. For light microscopy, 1  $\mu$ m sections were stained with 1 % toluidine blue in 1 % borax, while for transmission electron microscopy, 50 nm sections were collected on Formvar-coated slot copper grids and stained with saturated uranyl acetate in 50 % ethanol (30 min), then washed with 50 % ethanol followed by two changes of distilled water. They were further stained for 30 min in REYNOLDS lead citrate (24), washed with carbonate-free 0.02 M NaOH then with distilled water (twice). Stained sections were examined in a Philips EM 300 electron microscope.

Leaf samples of *V. riparia* were embedded in an alternative resin. After dehydration through alcohol as above the samples were placed in propylene oxide (2 changes, each of 10 min) then infiltrated with Taab epoxy medium (Taab Laboratories, Reading, U. K.) as for the SPURR resin. The resin was polymerised at 60 °C for 24–48 h.

Infected tissues of *V. vinifera* were examined at 3.5, 9, 16.5, 24, 40, 72 and 90 h following inoculation while those of *V. riparia* were examined at 3.5, 18, 24, 48, 72 and 96 h.

## Results and discussion

### Host Penetration

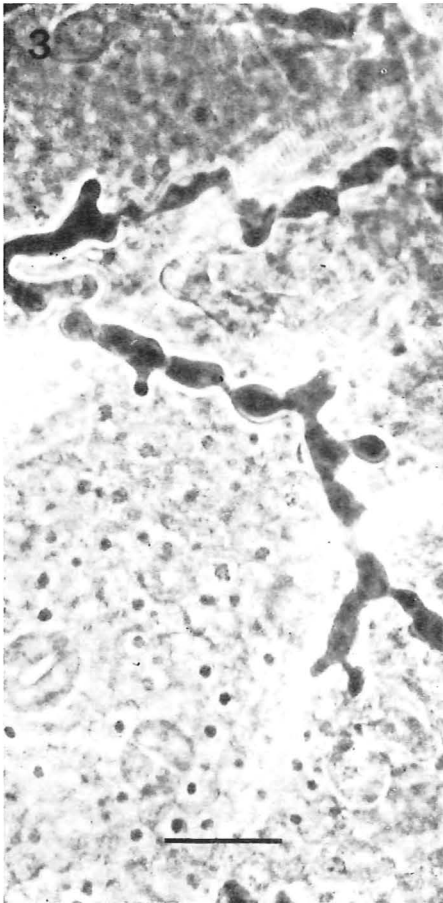
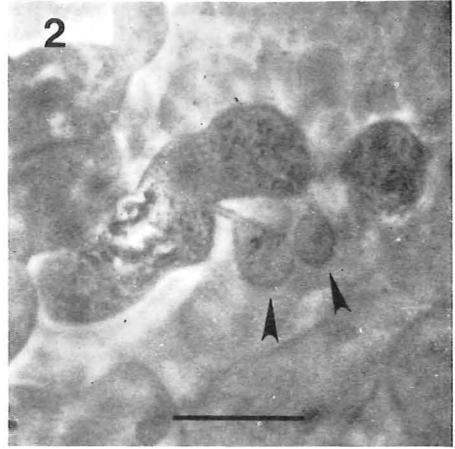
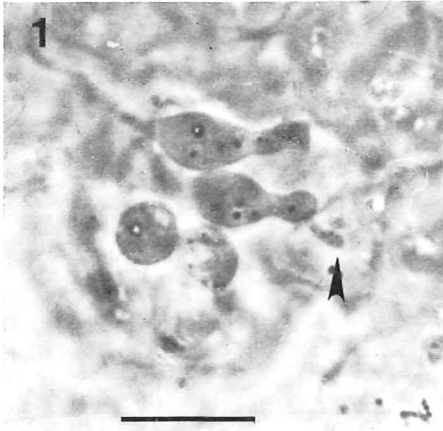
At no time during these experiments was the infection of grapevine by *P. viticola* seen to be initiated by sporangia except via the liberation of zoospores. This accords with previous observations of *P. viticola* (4, 26) and contrasts with *Bremia lactucae* in which infection almost always occurs by direct germination of sporangia (27). In *Phytophthora infestans* however, infection by either zoospores or sporangia is possible depending on environmental conditions (11). The release of zoospores from washed sporangia of *P. viticola* normally takes place within 30 min at room

temperature *in vitro*, and no induction process (e. g. cold shock as for *Ph. infestans*) is required for this. The release of zoospores on the leaf surface takes place with similar rapidity. The liberated zoospores congregate around open stomata to which they appear to be attracted, possibly in response to a gradient of increasing oxygen concentration, although, as discussed by ROYLE and THOMAS (26), other chemotactic stimuli appear to be involved. Once the zoospores have reached the vicinity of the stoma, where frequently four or five zoospores were seen to congregate, encystment takes place followed by the outgrowth of a single narrow germ tube from each encysted zoospore. The germ tube penetrates the stomatal aperture and, once inside the substomatal cavity, swells to form a substomatal vesicle (SSV). During this time, the cytoplasmic contents of the encysted zoospore pass into the SSV leaving empty ghosts of the encysted zoospores. Each SSV is derived from a single zoospore such that the substomatal cavity may contain four or five SSVs, the distal ends of which narrow to form a short hypha. At the tips of these hyphae, where they contact a mesophyll cell of the host, a haustorium may be initiated (Fig. 1). These processes are extremely rapid, the initiation of the first haustorium taking place within 3.5 h of application of a sporangial suspension to the abaxial surface of the leaf. The rapidity of the infection process may be a characteristic of biotrophic fungi of the order Peronosporales. Similarly rapid infection processes are observed in other members, e. g. *B. lactucae* (27), *Ph. infestans* (28) and *Peronospora parasitica* (7). By contrast, in *Puccinia graminis* (31) the first haustoria were not formed until 16 h after inoculation, and in necrotrophic fungi, e. g. *Piricularia oryzae* (6), host cell penetration may not occur for 24 h after inoculation. Sporangia, and in particular zoospores, of downy mildew fungi have limited resistance to desiccation as well as limited biosynthetic capability in the absence of host tissue and it is to the advantage of the parasite therefore that this vulnerable stage in its life history should be reduced to a minimum. Downy mildew fungi such as *B. lactucae* which have dispensed with the vulnerable zoospore stage are considered to be more highly evolved than e. g. *P. viticola* which is dependent on zoospores (11).

#### Colonisation of host tissue

Despite the speed of development of *P. viticola* in the first few hours, relatively little further development is normally seen for the succeeding 12–15 h. During this period no further hyphal development takes place although the haustorium is seen to increase in size considerably. It is likely that further development of the hyphae cannot take place until a fully developed and functional haustorium has been formed since the zoospore can contain only small amounts of stored reserves. Once the haustorium is fully developed, however, a phase of rapid growth of the fungus ensues. At 24 h after inoculation the hyphae have extended beyond the point at which the first haustorium was formed and additional haustoria are sometimes visible although hyphal branching may not have occurred as yet. At all times, the hyphae remain intercellular and they tend to fill the air spaces between the mesophyll cells of the host, thereby assuming a very irregular shape (Figs. 2 and 3). The inoculated area continues to become heavily invaded by the fungus (Fig. 4) which pushes its way up between palisade cells and may reach the upper epidermis of the leaf (Fig. 5). Further development of the SSVs also occurs so that the substomatal cavity may become totally occluded by these structures (Fig. 6).

Although the hyphae invade the tissue surrounding the inoculated area with apparent ease, vascular tissue is seen to present a considerable barrier to the spread of the fungus (Fig. 4). In young leaves, the fungus is able to breach this barrier in



one or two places enabling it to colonize the adjacent interveinal area and this frequently leads to the macroscopic appearance of confluent sporulation of the fungus. In more mature leaves, vascular tissue is less easily breached and individual lesions remain restricted to these interveinal areas.

### Sporulation

Hyphae which reach an uninvaded substomatal cavity may swell within this cavity, subsequently giving rise to sporangiophores which emerge through the stoma (Fig. 7). Initially, a single sporangiophore bearing numerous sporangia may develop but the initials of sporangiophores which may develop subsequently are also visible. Under the conditions of these experiments, sporulation occurred approx. 90 h after inoculation. An interesting feature of Fig. 7 is that the stomatal aperture appears to be completely covered by a thin septum, continuous with the cuticle. ROYLE and THOMAS (25) have reported similar septa in young stomata of hop. These septa are normally ruptured as the stoma develops.

### Ultrastructural features

**Mycelium.** — The ultrastructure of *P. viticola* as revealed by transmission electron microscopy has a similar general appearance to that of closely related fungi such as *Ph. infestans*, *B. lactucae* and *Pseudoperonospora humuli*. Subcellular components such as nuclei, nucleoli (Fig. 7), mitochondria (Fig. 8), ribosomes (Fig. 9), lomasomes (12) (Fig. 10) and Golgi bodies (Fig. 11) are clearly visible. The mycelium is aseptate. Extensive vacuolation of the mycelium is evident but the extent of this vacuolation varies with age of the hyphae. Young hyphae have relatively few vacuoles but the extent of vacuolation increases with age (Fig. 8) such that older

Infections of *V. vinifera* by *P. viticola*. Cleared whole leaf pieces, acid fuchsin stain, light microscopy.

Fig. 1: Substomatal vesicles with short hyphae developing from them. A haustorium (arrow) has been initiated. 3.5 h infection. Bar = 20  $\mu\text{m}$ .

Fig. 2: Intercellular mycelium developing from the substomatal cavity showing haustoria (arrows). 40 h infection. Bar = 20  $\mu\text{m}$ .

Fig. 3: Intercellular mycelium showing the irregular shape. Haustoria are not visible in this photograph. 40 h infection. Bar = 40  $\mu\text{m}$ .

Fig. 4: Extensive colonisation of the leaf in the upper part of the picture has occurred but invasion of the adjacent tissue is restricted by the large vascular bundle. The large crystalline deposits are raphides (calcium oxalate crystals contained within specialised cells) which are characteristic of vine leaves. 72 h infection. Bar = 100  $\mu\text{m}$ .

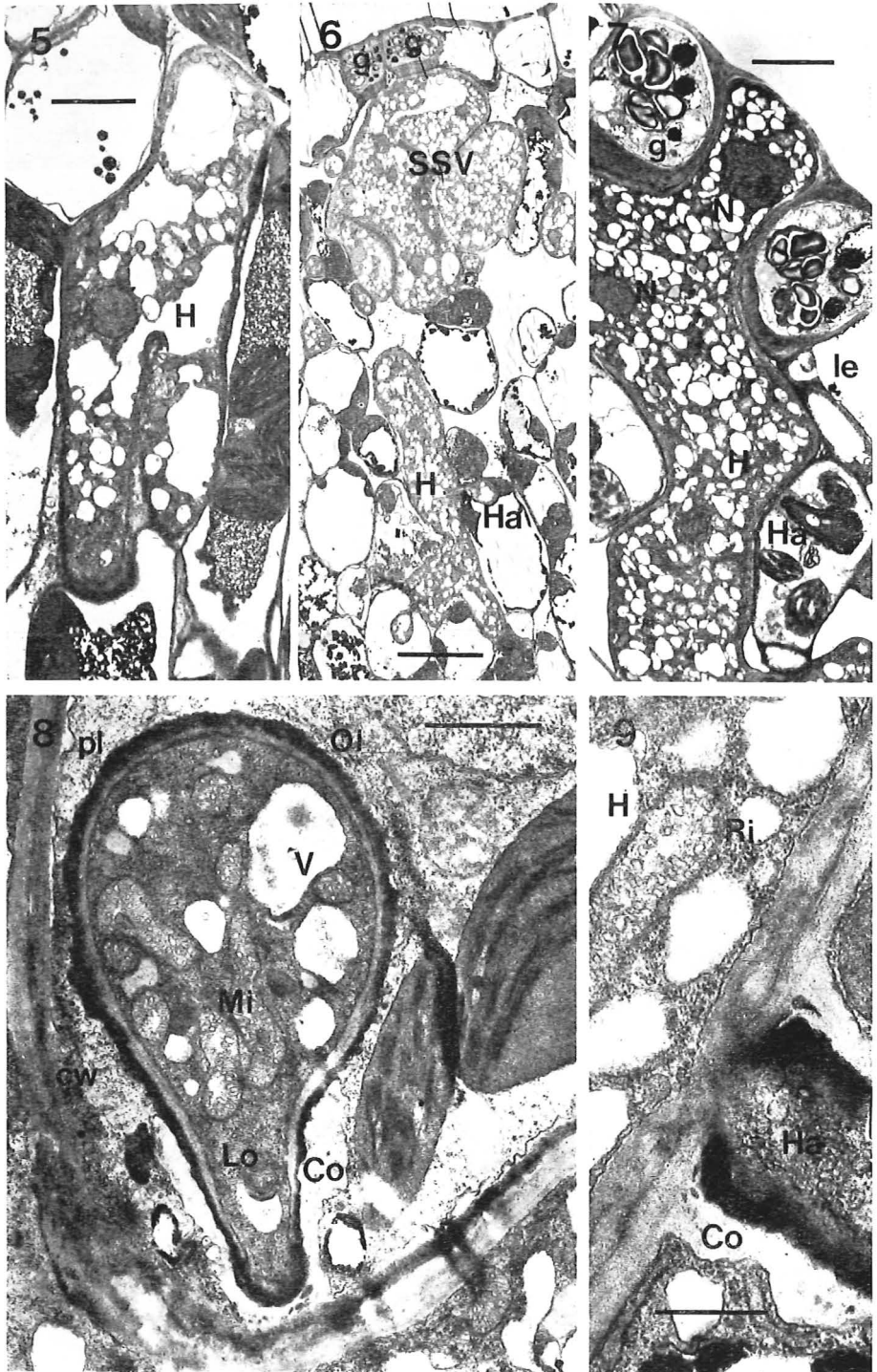
Infektion von *V. vinifera* durch *P. viticola*. Aufgehellte Blattstücke, Säurefuchsin-Färbung, Lichtmikroskopie.

Abb. 1: Substomatale Vesikel mit kurzen Hyphen, die sich aus ihnen entwickeln. Ein Haustorium (Pfeil) ist entstanden. 3,5stündige Infektion. Maßstab = 20  $\mu\text{m}$ .

Abb. 2: Interzelluläres Mycel, das sich von der Atemhöhle aus entwickelt und Haustorien (Pfeile) zeigt. 40stündige Infektion. Maßstab = 20  $\mu\text{m}$ .

Abb. 3: Interzelluläres Mycel, das die typische unregelmäßige Form zeigt. In dieser Aufnahme sind keine Haustorien zu sehen. 40stündige Infektion. Maßstab = 40  $\mu\text{m}$ .

Abb. 4: Im oberen Teil des Präparates ist eine ausgedehnte Pilzbesiedlung erfolgt, im anschließenden Gewebe wurde das Eindringen des Mycels jedoch durch das große Gefäßbündel unterbunden. Bei den großen Kristallablagerungen handelt es sich um Raphiden (Einschlüsse von Calciumoxalatkristallen in spezialisierten Zellen), die für Rebenblätter charakteristisch sind. 72stündige Infektion. Maßstab = 100  $\mu\text{m}$ .



Infections of *V. vinifera* by *P. viticola*. Transmission electron micrographs.

Fig. 5: Hyphe (H) in the palisade layer of the leaf. 90 h infection. Bar = 2.5  $\mu\text{m}$ .

Fig. 6: General view of an infection site showing proliferation of substomatal vesicles (SSV) and hyphae invading the surrounding tissue. 90 h infection. Bar = 10  $\mu\text{m}$ .

Fig. 7: Sporangiphore emerging through stoma. Note that the stomatal aperture is covered by a thin septum continuous with the cuticle. 90 h infection. Bar = 2.5  $\mu\text{m}$ .

Fig. 8: Non-median section through haustorium and part of haustorial neck. The neck is surrounded by an electron translucent collar (Co) which has been deposited on the host cell wall (cw) outside the host plasmalemma (pl), thereby invaginating it. At the inner end of the collar the host plasmalemma merges with the osmiophilic layer (Ol) which characteristically surrounds the haustoria. There is a membranous vesicular structure (lomasome, Lo) in the neck region of the haustorium which contains many mitochondria (Mi) and vacuoles (V). 90 h infection. Bar = 1  $\mu\text{m}$ .

Fig. 9: Non-median section through the haustorial neck. Membranes of both host and fungus are particularly clear in this picture as are the collar (Co) and fungal ribosomes (Ri). 90 h infection. Bar = 0.5  $\mu\text{m}$ .

#### Abbreviations:

##### Fungal Structures

Co — Collar  
Cw — Cell wall  
Er — Endoplasmic reticulum  
Go — Golgi apparatus  
H — Intercellular hypha  
Ha — Haustorium  
Lo — lomasome

Mi — Mitochondrion  
N — Nucleus  
Nu — Nucleolus  
Ol — Osmiophilic layer  
Ri — Ribosome  
SSV — Substomatal vesicle  
V — Vacuole

##### Host structures

c — Chloroplast  
cw — Cell wall  
cy — Cytoplasm  
g — Guard cell  
le — Lower epidermis  
pl — Plasmalemma  
t — Tonoplast

#### Infektion von *V. vinifera* durch *P. viticola*. Transmissions-elektronenmikroskopische Aufnahmen.

Abb. 5: Hyphe (H) in der Palisadenschicht des Blattes. 90stündige Infektion. Maßstab = 2,5  $\mu\text{m}$ .

Abb. 6: Übersichtsbild einer Infektionsstelle mit auswachsenden substomatalen Vesikeln (SSV) und Hyphen, die in das umgebende Gewebe eindringen. 90stündige Infektion. Maßstab = 10  $\mu\text{m}$ .

Abb. 7: Sporangienträger beim Verlassen eines Stomas. Zu beachten ist, das die Spaltöffnung von einem dünnen Septum bedeckt ist, das in die Cuticula übergeht. 90stündige Infektion. Maßstab = 2,5  $\mu\text{m}$ .

Abb. 8: Nichtmedianer Schnitt durch ein Haustorium und einen Teil seines Halses. Der Hals wird von einem elektronendurchlässigen Kragen (Co) umgeben, der auf der Wirtszellwand (cw), außerhalb des Plasmalemmas (pl), abgelagert wurde und dieses dabei einstellte. Am inneren Rande des Kragens verschmilzt das Wirtsplasmalemma mit der osmiophilen Schicht (Ol), welche die Haustorien in charakteristischer Weise umgibt. In der Halsregion des Haustoriums findet sich eine membranöse und blasige Struktur (Lomasom, Lo), die zahlreiche Mitochondrien (Mi) und Vakuolen (V) enthält. 90stündige Infektion. Maßstab = 1  $\mu\text{m}$ .

Abb. 9: Nichtmedianer Schnitt durch den Haustoriumshals. Die Zellmembranen sowohl des Wirtes wie des Pilzes sind auf diesem Bild besonders deutlich, ebenso der Kragen (Co) und die Ribosomen des Pilzes (Ri). 90stündige Infektion. Maßstab = 0,5  $\mu\text{m}$ .

#### Abkürzungen:

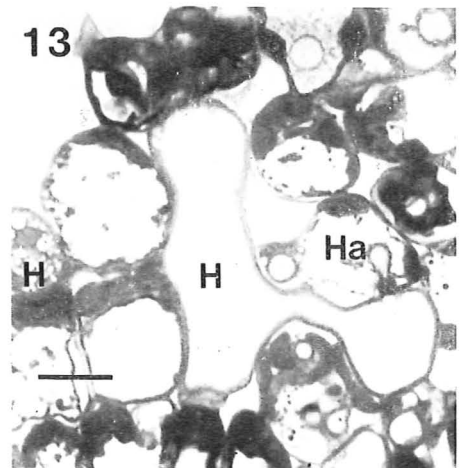
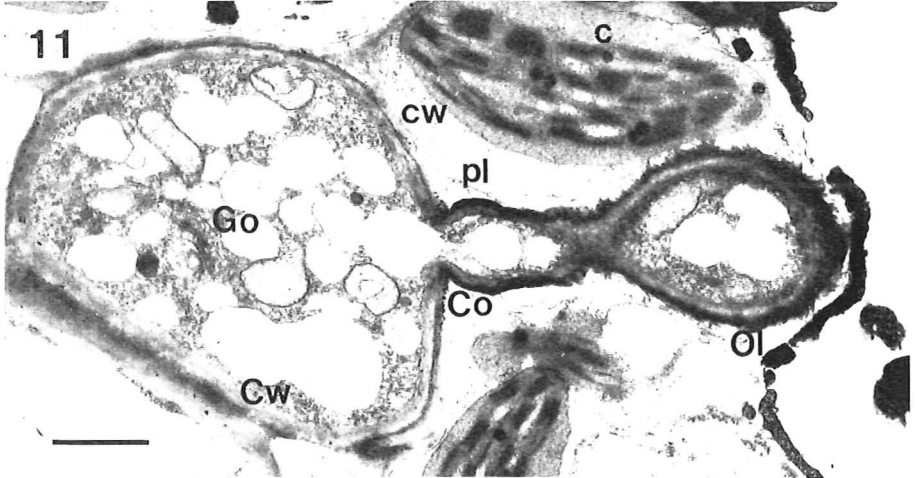
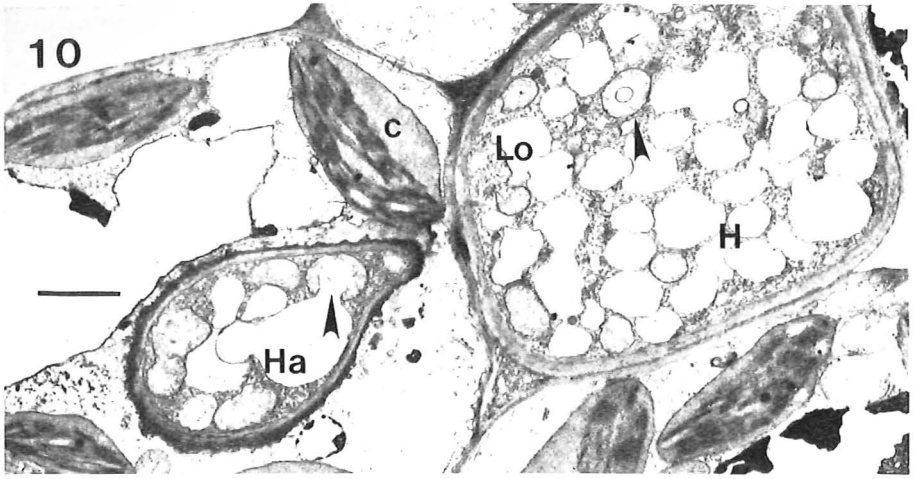
##### Strukturen des Pilzes

Co — Kragen  
Cw — Zellwand  
Er — Endoplasmatisches Reticulum  
Go — Golgiapparat  
H — Intercellulare Hyphe  
Ha — Haustorium  
Lo — Lomasom

Mi — Mitochondrium  
N — Zellkern  
Nu — Nucleolus  
Ol — Osmiophile Schicht  
Ri — Ribosom  
SSV — Substomatale Vesikel  
V — Vakuole

##### Strukturen des Wirtes

c — Plasmalemma  
cw — Tonoplast  
cy — Chloroplast  
g — Zellwand  
le — Cytoplasma  
pl — Schließzelle  
t — Untere Epidermis





portions of the fungus, including haustoria, may be totally devoid of cytoplasm (Fig. 13). Similar observations have been made in the downy mildew diseases of both hop (21) and lettuce (13), and a similar process frequently occurs in culture with fungi of this order (11).

**H a u s t o r i a .** — The nature of the haustoria is of particular interest since these represent the true host-parasite interface through which the exchange of metabolites between host and pathogen occurs (5). The haustoria are typically pear-shaped (Figs. 8, 10, 11). The fungal cell wall is continuous with the haustorial wall and both appear to be of similar structure. There is a conspicuous electron-dense layer surrounding the cell wall of the haustoria (Figs. 8, 10, 11) and this is not seen to continue around the cell wall of the intercellular hyphae. A similar electron-dense layer is evident around haustoria of other downy mildew fungi (7, 13, 21, 23) but this is not

#### Infections of *V. vinifera* by *P. viticola*

Fig. 10: Electron micrograph of transverse section of intercellular mycelium (H) with part of a haustorium (Ha) in the adjacent mesophyll cell of the host. Several invaginated mitochondria (arrowed) are visible in the fungus. 90 h infection. Bar = 2.5  $\mu\text{m}$ .

Fig. 11: Electron micrograph of near-median section through haustorium and haustorial neck. As in Fig. 10, parts of the host plasmalemma (pl) can be traced inside the host cell wall (cw) and surrounding the collar (Co) but it cannot be distinguished around the osmiophilic layer (Ol). The fungal cell wall (Cw) is continuous with the cell wall surrounding the haustorium. Golgi apparatus (Go) can be seen in the intercellular hypha. 90 h infection. Bar = 1  $\mu\text{m}$ .

Fig. 12: Electron micrograph of section through substomatal cavity showing substomatal vesicles (SSV) and mycelium (H) which has developed from them. 90 h infection. Bar = 5  $\mu\text{m}$ .

Fig. 13: Light micrograph of sectioned material showing a large area of intercellular mycelium (H), with a haustorium (Ha), devoid of cytoplasm. A section of an intercellular hypha containing cytoplasm with numerous small vacuoles can also be seen to the left. 90 h infection. Bar = 15  $\mu\text{m}$ .

Further abbreviations see Figs. 5—9.

#### Infektion von *V. vinifera* durch *P. viticola*.

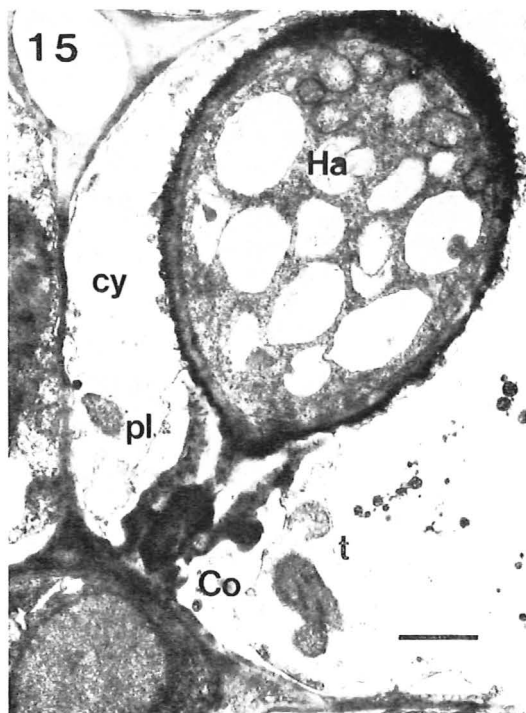
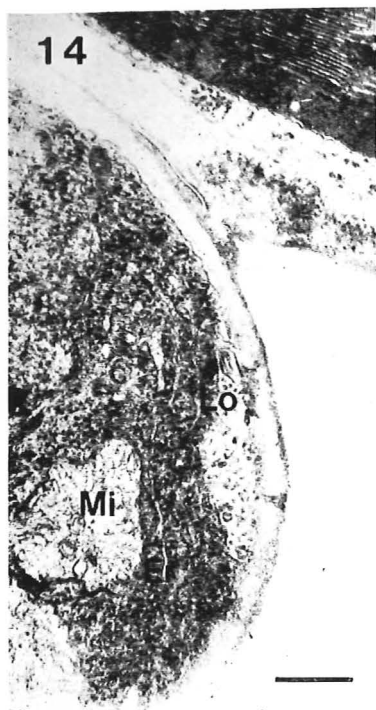
Abb. 10: Elektronenmikroskopische Aufnahme eines quergeschnittenen intercellularen Myceliums (H) mit Teil eines Haustoriums (Ha) in der benachbarten Mesophyllzelle der Wirtspflanze. Im Pilz sind etliche eingedellte Mitochondrien (Pfeile) zu erkennen. 90-stündige Infektion. Maßstab = 2,5  $\mu\text{m}$ .

Abb. 11: Elektronenmikroskopische Aufnahme eines paramedianen Schnittes durch ein Haustorium und dessen Hals. Wie in Abb. 10 können Teile des Wirtsplasmalemmas (pl) innerhalb der Wirtszellwand (cw) verfolgt werden; das Wirtsplasmalemma umgibt den Kragen (Co), hebt sich aber im Bereich der osmiophilen Schicht (Ol) nicht mehr ab. Die Pilzzellwand (Cw) setzt sich in die das Haustorium umgebende Zellwand fort. In der intercellularen Hyphe ist ein Golgiapparat (Go) zu sehen. 90stündige Infektion. Maßstab = 1  $\mu\text{m}$ .

Abb. 12: Elektronenmikroskopische Aufnahme eines Schnittes durch eine Atemhöhle mit substomatalen Vesikeln (SSV) und Mycel (H), das sich aus diesen entwickelt hat. 90-stündige Infektion. Maßstab 5  $\mu\text{m}$ .

Abb. 13: Lichtmikroskopische Aufnahme eines Schnittes, der einen ausgedehnten Bezirk intercellularen Mycels sowie ein Haustorium zeigt, die frei von Cytoplasma sind. Eine angeschnittene intercellulare Hyphe, die Cytoplasma mit zahlreichen kleinen Vakuolen enthält, kann links im Bilde ebenfalls erkannt werden. 90stündige Infektion. Maßstab = 15  $\mu\text{m}$ .

Weitere Abkürzungen bei Abb. 5—9.



present around haustoria of powdery mildews and rusts although various other forms of encapsulation may be present (5). In *P. parasitica*, CHOU (7) suggested that this osmiophilic layer, which corresponds with the zone of apposition of PEYTON and BOWEN (23), is a continuation of a thin electron-dense layer around intercellular hyphae. The neck of the haustorium is surrounded by a collar which surrounds the electron dense layer in this region (Figs. 8, 9). By analogy with similar structures, which have been observed in other downy mildew infections (13, 21, 23), it is presumed that this collar consists principally of callose, a  $\beta$ -1,3 linked glucan typically produced as a wound response. This collar was invariably present with *P. viticola* although it is not always found in other downy mildews e. g. *P. humuli* (21).

In the rusts and powdery mildews it has clearly been established that the haustoria invaginate the host cytoplasm (5). The continuity of the host plasmalemma around the haustorium can be detected. Among the downy mildews there may be species differences on this point. INGRAM *et al.* clearly state that the host plasmalemma is continuous around haustoria of *B. lactucae* where it is closely adpressed to the electron-dense layer (13). On the other hand, ASADA and SHIRAISHI claim that the plasmalemma of the radish host is ruptured by haustoria of *P. parasitica* (2). The situation in *P. viticola* appears to be similar to that of *P. parasitica* in that the host plasmalemma can be traced beneath the host cell wall and around the collar

Infections of *V. vinifera* by *P. viticola*. Transmission electron micrographs.

Fig. 14: Typical lomasome (Lo) in an intercellular hypha. Endoplasmic reticulum (Er) and mitochondria (Mi) are evident. 16.5 h infection. Bar = 0.25  $\mu$ m.

Fig. 15: Non-median section of haustorium (Ha) and adjacent intercellular hypha. Host cytoplasm (cy) is present as a thin layer around the haustorial head. This is the most common appearance of the haustoria in *V. vinifera*. 90 h infection. Bar = 1  $\mu$ m.

Fig. 16: Median section of haustorium. The host cell cytoplasm has severely degenerated although the cytoplasm of both the haustorium and the intercellular hyphae appears relatively normal. 90 h infection. Bar = 1  $\mu$ m.

Fig. 17: Median section of haustorium which has collapsed. The host cell cytoplasm is not normal although it has not degenerated as severely as in the example of Fig. 16. The cytoplasm of the intercellular hypha (H) appears to be normal. 90 h infection. Bar = 1  $\mu$ m.

Further abbreviations see Figs. 5–9.

Infektion von *V. vinifera* durch *P. viticola*, Transmissionselektronenmikroskopische Aufnahmen.

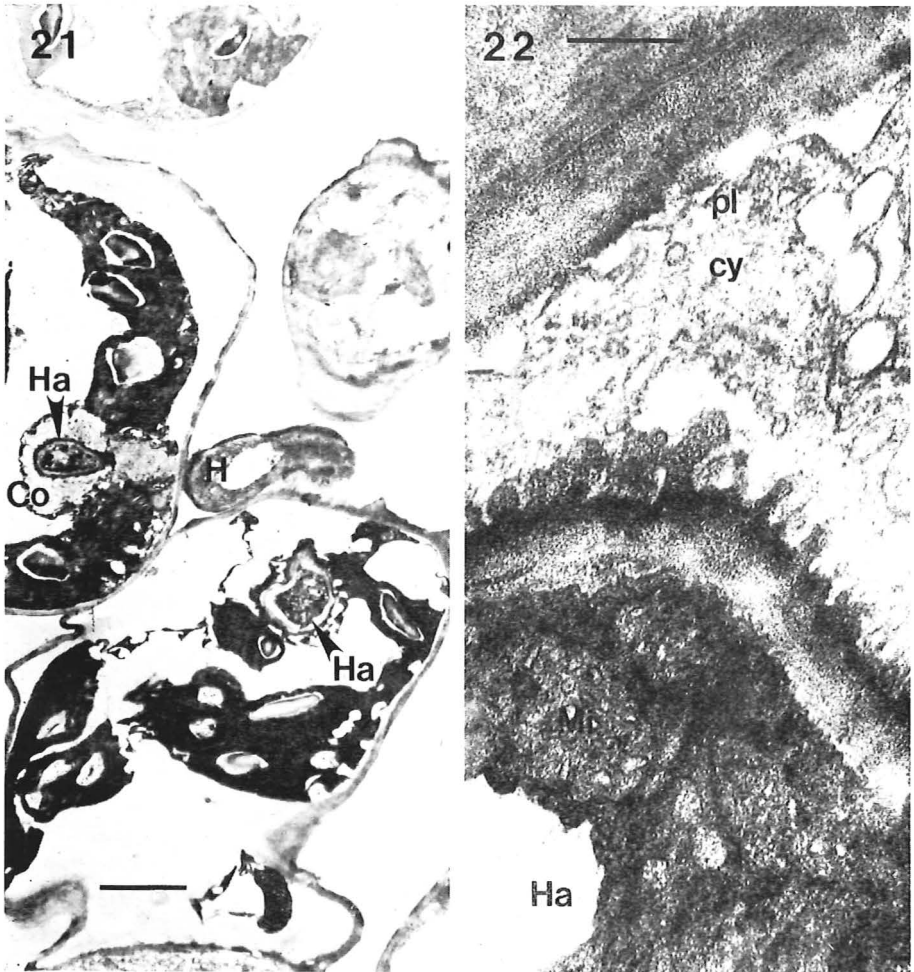
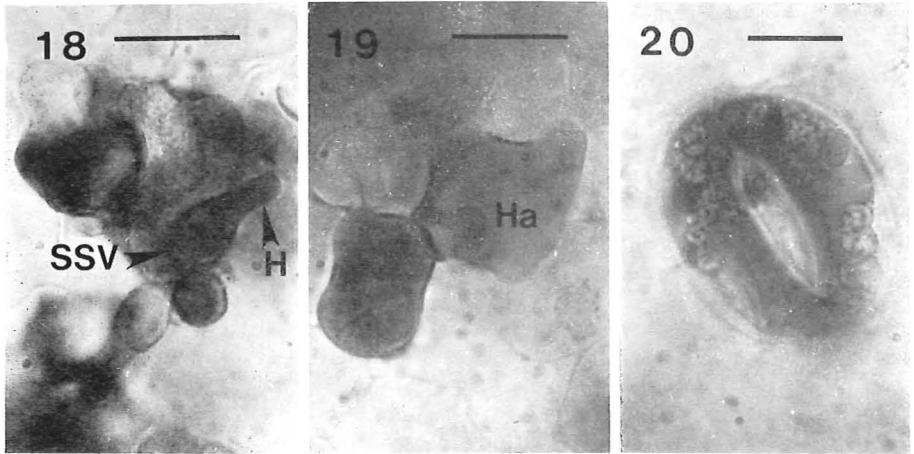
Abb. 14: Typisches Lomasom (Lo) in einer intercellularen Hyphe. Deutlich zu erkennen sind das endoplasmatische Reticulum (Er) und Mitochondrien (Mi). 16,5stündige Infektion. Maßstab = 0,25  $\mu$ m.

Abb. 15: Nichtmedianer Schnitt durch ein Haustorium und die anschließende intercellulare Hyphe. Das Wirtscytoplasma umgibt als dünne Schicht den Kopf des Haustoriums. Dies ist das häufigste Erscheinungsbild der Haustorien bei *V. vinifera*. 90stündige Infektion. Maßstab = 1  $\mu$ m.

Abb. 16: Medianschnitt durch ein Haustorium. Das Cytoplasma der Wirtszelle ist stark degeneriert, während das Cytoplasma sowohl von Haustorium wie von intercellularer Hyphe relativ normal erscheint. 90stündige Infektion. Maßstab = 1  $\mu$ m.

Abb. 17: Medianschnitt durch ein kollabiertes Haustorium. Das Cytoplasma der Wirtszelle ist nicht normal, obgleich es nicht so stark degeneriert ist wie im Falle von Abb. 16. Das Cytoplasma der intercellularen Hyphe (H) wirkt normal. 90stündige Infektion. Maßstab = 1  $\mu$ m.

Weitere Abkürzungen bei Abb. 5–9.



surrounding the haustorial neck (Fig. 9). At the inner end of the collar however, it becomes merged with the electron dense layer (Figs. 8, 10, 11; cf. Fig. 3 of (2)) and there is no clear evidence of the presence of the plasmalemma around the remainder of the haustorium. FARINA *et al.* (9) were similarly unable to trace the host plasmalemma around haustoria of *P. viticola* in grapevine. Although this would suggest that the plasmalemma is ruptured, it is possible that it is so closely associated with

Infections of *V. riparia* by *P. viticola*. Figs. 18, 19 and 20: Cleared whole leaf pieces, trypan blue stain, light microscopy.

Fig. 18: Substomatal vesicles (SSV) with short hyphae (H). Necrotic (hypersensitive) responses of the mesophyll cells adjacent to fungal hyphae have occurred. Some of these mesophyll cells were seen to contain haustoria although this is not evident from the photograph. 48 h infection. Bar = 20  $\mu\text{m}$ .

Fig. 19: Small haustorium (Ha) in a hypersensitive mesophyll cell at edge of substomatal cavity. 24 h infection. Bar = 20  $\mu\text{m}$ .

Fig. 20: Hypersensitive reaction of guard cells of stoma. 24 h infection. Bar = 20  $\mu\text{m}$ .

Fig. 21: Electron micrograph of hypersensitive responses of mesophyll cells containing haustoria. The contents of the two hypersensitive mesophyll cells have degenerated severely and appear plasmolysed, while the neighbouring mesophyll cell (top) appears unaffected. The fungal cytoplasm within the haustoria has severely degenerated and there is an extensive collar around both haustoria. 24 h infection. Bar = 2.5  $\mu\text{m}$ .

Fig. 22: Electron micrograph of a mesophyll cell containing a haustorium. The host cytoplasm appears to be normal. Fungal cytoplasm in the haustorium shows some degenerative changes. Fingerlike projections of the osmiophilic layer occur in the host cytoplasm. Even at this magnification there is no clear evidence of the host plasmalemma surrounding the haustorium although the host plasmalemma (pl) can be detected in other places. 48 h infection. Bar = 0.2  $\mu\text{m}$ .

Further abbreviations see Figs. 5–9.

Infektion von *V. riparia* durch *P. viticola*. Abb. 18, 19 und 20: Aufgehellte Blattstücke, Trypanblau-Färbung, Lichtmikroskopie.

Abb. 18: Substomatale Vesikel (SSV) mit kurzen Hyphen (H). In den Mesophyllzellen, die den Pilzhypen benachbart sind, erfolgen nekrotische (hypersensitive) Reaktionen. In einigen dieser Mesophyllzellen wurden Haustorien vorgefunden (aus der Aufnahme nicht ersichtlich). 48stündige Infektion. Maßstab = 20  $\mu\text{m}$ .

Abb. 19: Kleines Haustorium (Ha) in einer hypersensitiven Mesophyllzelle am Rande der Atemhöhle. 24stündige Infektion. Maßstab = 20  $\mu\text{m}$ .

Abb. 20: Überempfindlichkeitsreaktion der Stomaschließzellen. 24stündige Infektion. Maßstab = 20  $\mu\text{m}$ .

Abb. 21: Elektronenmikroskopische Aufnahme der Überempfindlichkeitsreaktion von Mesophyllzellen, die Haustorien enthalten. Der Inhalt der beiden hypersensitiven Mesophyllzellen ist stark degeneriert und wirkt plasmolysiert, während die benachbarte Mesophyllzelle (oben) unbeeinflusst erscheint. Das Pilzcytoplasma ist in den Haustorien stark degeneriert, und um beide Haustorien legt sich ein umfangreicher Kragen. 24stündige Infektion. Maßstab = 2,5  $\mu\text{m}$ .

Abb. 22: Elektronenmikroskopische Aufnahme einer Mesophyllzelle mit einem Haustorium in ihrem Inneren. Das Wirtscytoplasma wirkt normal. Das Pilzcytoplasma im Haustorium zeigt einige degenerative Veränderungen. Im Wirtscytoplasma treten fingerartige Fortsätze der osmiophilen Schicht auf. Selbst bei der vorliegenden Vergrößerung läßt sich das Wirtsplasmalemma in der Umgebung des Haustoriums nicht eindeutig nachweisen, während es an anderen Stellen (pl) in Erscheinung tritt. 48stündige Infektion. Maßstab = 0,2  $\mu\text{m}$ .

Weitere Abkürzungen bei Abb. 5–9.

the electron-dense layer that it would not be detectable. This is confirmed by the recent studies of PARES and GREENWOOD (22) who showed that the peri-haustorial membrane of *P. humuli* can best be seen using a tilting stage in the electron microscope.

Haustoria of *P. viticola* are rich in mitochondria and ribosomes (Fig. 8) as are haustoria of other pathogens and this would be expected of a region presumed to have high metabolic activity. Mitochondria, however, are also very frequent in the intercellular mycelium. In some cases they have an invaginated appearance (Fig. 10) as described by PARES and GREENWOOD (21). Structures resembling those described by others (e. g. 13) as lomasomes occur both in the haustorial neck region where they are quite frequently, though not invariably, seen, and in other regions of the intercellular hyphae where they are closely adpressed to the fungal cell wall (Fig. 14). HEATH and GREENWOOD (12) considered lomasomes to be regions in which membrane synthesis was in excess of requirements. Vesicular structures are also present in the host cytoplasm (Fig. 8), particularly in association with the collar around the haustorial neck. At no time were the haustoria of *P. viticola* seen to contain nuclei. Once again, there may be species differences here among the Peronosporales on this point. Nuclei are present in haustoria of both *P. parasitica* (7) and *B. lactucae* (13) but are absent from those of *Albugo candida* (3) and *Pseudoperonospora* spp. (21, 15). In the higher fungi, nuclei are typically found in haustoria of both the rusts and the powdery mildews (5). Unlike haustoria of the powdery mildews, the haustoria of most fungi, including *P. viticola*, are not cut off from the rest of the mycelium by a septum in the neck region.

#### Host responses to infection

No consistent responses of the host cells to invasion by haustoria of *P. viticola* were seen. Although *P. viticola* shows primitive disease characteristics in that infection ultimately leads to gross necrosis of the leaves and defoliation, the pathogen shows considerably more adaptation to the parasitic mode than does its relative *Ph. infestans* since a balanced coexistence between host and parasite may be maintained for several days following infection. Under the conditions used in these experiments, which were near optimal for disease development, adverse effects of the pathogen on the host were not seen, either macroscopically or in cleared leaf segments until sporulation occurred (4–5 d after inoculation). At this time, a hypersensitive type of browning response of small groups of cells was seen although this was always towards the centre of a lesion, the region in which the fungus had been in contact with host cells for the longest. Ultrastructurally, a range of reaction types were seen among host cells. In many cells there was no obvious reaction of the host cell to the presence of the haustorium. The host cytoplasm was present as a thin layer surrounding the haustorium and projecting into the host vacuole (Fig. 15). This is probably the normal situation in newly formed haustoria. The deposition of osmium stain in the vacuoles of the host cells, either as amorphous dense black globules close to the tonoplast (Figs. 9, 10, 11) or as a more general granular appearance in the vacuoles (Fig. 5) was frequently seen in cells containing haustoria, but examination of non-infected tissue showed that this frequently occurs in normal cells, particularly in those of the palisade layer. This is presumably due to the presence of phenolic materials.

A frequent response of host cells was a general proliferation of the cytoplasm. Normal mesophyll cells contain a thin layer of cytoplasm beneath the cell wall and surrounding the vacuole, but in many cells containing haustoria, the vacuole was much reduced in size or even absent, the difference being accounted for by the

increased volume of host cytoplasm (Figs. 8, 10). At the later stages of infection, two types of response were evident. In some cells, the host cytoplasm degenerated while the haustorium retained its normal appearance (Fig. 16). This is very similar to the ultrastructural appearance of hypersensitively responding cells as shown by INGRAM *et al.* (13). In other cells, the host cytoplasm had not totally degenerated but the haustorium had collapsed (Fig. 17). The adjacent intercellular hypha remained apparently healthy.

#### Infection of *V. riparia* by *P. viticola*

*V. riparia* is resistant to both *Botrytis cinerea* and *P. viticola*. BOUBALS (4) classified it as having reaction type I to *P. viticola*, in which infection results in small depressions in the leaf surface where small brown necroses of and around the stomata are evident. Sporangia are only produced under conditions highly favourable for infection (e. g. continuous high R. H.) and even then they are few in number. Similar reactions were seen in the present study. Microscopic observation showed that on leaves of *V. riparia* sporangia liberate their zoospores, the zoospores congregate around stomata, encyst and germinate. The germ tubes penetrate stomata and form SSVs in the substomatal cavity (Fig. 18). A haustorium is formed at the tip of the hypha developing from the SSV (Fig. 19). There were no differences in these events occurring in leaves of *V. riparia* as compared with *V. vinifera* up to approximately 18 h following inoculation. Subsequent development in *V. riparia* was severely curtailed, although not completely, and there were differences in the extent of further development that occurred at different infection sites, even within the same leaf. At most infection sites, there was no further fungal growth up to 4 d following inoculation, at which stage the study was terminated. At other infection sites, a hypha would continue to grow intercellularly with the occasional formation of haustoria. These intercellular hyphae tended to be straighter and less irregular in shape than in *V. vinifera*, and there was very little hyphal branching.

Necrotic browning (hypersensitive) reactions of host cells were evident in cleared leaf segments. Occasionally they were evident as early as 24 h after inoculation but they were much more prevalent at 48 h. These responses initially occurred most frequently in one or both guard cells of the stomata (Fig. 20) even though penetration of guard cells themselves by hyphae or haustoria was never seen in either *V. riparia* or *V. vinifera*. Subsequently, necrosis of one or more mesophyll cells was seen particularly in those containing haustoria (Fig. 18). Some mesophyll cells, however, became necrotic even though penetration could not be seen while other cells containing haustoria did not become necrotic for at least 48 h after inoculation. It was clear, therefore, that hyphal development had been affected at many infection sites before the hypersensitive responses of host cells were evident as a gross disorganisation, granulation and browning of the cytoplasm. Macroscopically, the hypersensitive response could be seen between 2 and 3 d after infection.

Examination of the infection of *V. riparia* in the electron microscope proved to be more difficult. This was due to the greater difficulty in sectioning tissue of *V. riparia* and to the use of a non-carcinogenic, but less effective, embedding resin. In addition, because the volume of host tissue affected by the fungus was so much less than in *V. vinifera*, there was more difficulty in locating infection sites. Nevertheless, the hypersensitive reaction of guard cells and mesophyll cells containing haustoria (Fig. 21) could be seen. In some cases, an ensheathment of the haustorium by the material (callose) normally deposited as a collar around the neck was evident. In other mesophyll cells, the haustoria and host cytoplasm appeared to be relatively unaffected (Fig. 22).

Hypersensitive reactions of the sort described here are very commonly associated with resistance of many plants to disease. In addition, they are often associated with phytoalexin production. There is considerable controversy as to whether hypersensitivity and phytoalexin production are the cause or consequence of resistance (16, 20). However, it has been found that phytoalexins accumulate in *V. riparia* at about the same time as fungal development is inhibited (P. LANGCAKE, in preparation). It seems likely, therefore, that the inhibition of fungal growth in *V. riparia* can be accounted for by the accumulation of phytoalexins and that substantial amounts of phytoalexin production may occur before there is gross necrosis of the cells producing them. The host cell necrosis could then be a result of the phytotoxic concentrations of phytoalexins which accumulate, there being evidence for the phytotoxicity of certain phytoalexins (19, 30, 32).

### Summary

The infection of the susceptible grapevine species, *Vitis vinifera* L., and the resistant species, *V. riparia* MICHX., by the downy mildew pathogen, *Plasmopara viticola*, has been studied by light and electron microscopy. The infection cycle and ultrastructural features of the disease are described in detail and compared with those of other host-pathogen interactions.

We would like to thank Dr. F. A. WILLIAMSON for preparing the photographs and criticising the manuscript.

### References

1. AMICI, A., BALDACCIO, E. e MINERVINI, G., 1968: Sulla struttura e sulla modalita di penetrazione dell' austerio di *Plasmopara viticola* in *Vitis vinifera*. Riv. Pat. Veg. 4, 165—184.
2. ASADA, Y. and SHIRAIISHI, M., 1976: Discontinuity of the plasma membrane around haustoria of *Peronospora parasitica*. In: TOMIYAMA, K., DALY, J. M., URITANI, I., OKU, H. and OUCHI, S. (Eds.): Biochemistry and cytology of plant-parasite interaction, 32—34. Kodansha Ltd., Tokyo and Elsevier, Amsterdam.
3. BERLIN, J. D. and BOWEN, C. C., 1964: The host-parasite interface of *Albugo candida* in *Raphanus sativus*. Amer. J. Bot. 51, 445—452.
4. BOUBALS, D., 1959: Contribution à l'étude des causes de la résistance des Vitacées au mildiou de la vigne (*Plasmopara viticola* (B. et C.) BERL. et DE T.) et de leur mode de transmission héréditaire. Ann. de l'Amélior. Plantes 1, 1—236.
5. BRACKER, C. E. and LITTLEFIELD, L. J., 1973: Structural concepts of host-pathogen interfaces. In: BYRDE, R. J. W. and CUTTING, C. V. (Eds.): Fungal pathogenicity and the plant's response, 159—318. Academic Press, London.
6. CARTWRIGHT, D., 1978: Studies on the mode of action of the dichlorocyclopropane fungicides on rice blast disease. Ph. D. Thesis, University of Birmingham, U. K.
7. CHOU, C. K., 1970: An electron microscope study of host penetration and early stages of haustorium formation of *Peronospora parasitica* (Fr.) TUL. on cabbage leaves. Ann. Bot. 34, 189—204.
8. EHRLICH, M. A. and EHRLICH, H. G., 1966: Ultrastructure of the hyphae and haustoria of *Phytophthora infestans* and hyphae of *P. parasitica*. Canad. J. Bot. 44, 1495—1504.
9. FARINA, G., BARBIERI, N., BASSI, M. and BETTO, E., 1976: *Plasmopara viticola* in leaves of *Vitis vinifera*. An electron microscopic study. Riv. Pat. Veg. 12, 43—51.
10. GALBIATI, C., 1976: Lo sviluppo del micelio di *Plasmopara viticola* osservato al microscopio ottico in tessuti non sezionati di *Vitis vinifera*. Riv. Pat. Veg. 12, 34—42.
11. HAWKER, L. E., 1966: Fungi. Hutchinson University Library, London.



12. HEATH, I. B. and GREENWOOD, A. D., 1970: The structure and formation of lomasomes. *J. Gen. Microbiol.* 62, 129—137.
13. INGRAM, D. S., SARGENT, J. A. and TOMMERUP, I. C., 1976: Structural aspects of infection by biotrophic fungi. In: FRIEND, J. and THRELFALL, D. R. (Eds.): *Biochemical aspects of plant-parasite relationships*, 43—78. Academic Press, London.
14. JONES, D. R. and DEVERALL, B. I., 1977: The effect of the Lr20 resistance gene in wheat on the development of leaf rust, *Puccinia recondita*. *Physiol. Plant. Pathol.* 10, 275—284.
15. KAJIWARA, T., 1969: Ultrastructure of the host-parasite relationships in cucumber downy mildew caused by *Pseudoperonospora cubensis* (BERK. et CURT.) ROSTOW. *Bull. Natl. Inst. Agric. Sci.*, Ser. C, No. 23, 63—91.
16. KIRALY, Z., BARNA, B. and ERSEK, T., 1972: Hypersensitivity as a consequence, not the cause, of plant resistance to infection. *Nature* 239, 456—458.
17. LANGCAKE, P. and PRYCE, R. J., 1977: A new class of phytoalexins from grapevines. *Experientia* 33, 151—152.
18. LOCCI, R., 1969: Direct observation by scanning electron microscopy of the invasion of grapevine leaf tissues by *Plasmopara viticola*. *Riv. Pat. Veg.* 5, 199—206.
19. LYON, G. D. and MAYO, M. A., 1978: The phytoalexin rishitin affects the viability of isolated plant protoplasts. *Phytopathol.* Z. 92, 298—304.
20. MACLEAN, D. J., SARGENT, J. A., TOMMERUP, I. C. and INGRAM, D. S., 1974: Hypersensitivity as the primary event in resistance to fungal parasites. *Nature* 249, 186—187.
21. PARES, R. D. and GREENWOOD, A. D., 1977: Ultrastructure of the host-parasite relationships of *Pseudoperonospora humuli* on hops. *Austral. J. Bot.* 25, 585—598.
22. — — and — — , 1979: The periaustorial membrane in hop cells infected by *Pseudoperonospora humuli*. *New Phytol.* 83, 473—477.
23. PEYTON, G. A. and BOWEN, C. C., 1963: The host-parasite interface of *Peronospora manschurica* on *Glycine max*. *Amer. J. Bot.* 50, 787—797.
24. REYNOLDS, E. G., 1963: The use of lead citrate at high pH as an electron opaque stain in electron microscopy. *J. Cell Biol.* 17, 208—212.
25. ROYLE, D. J. and THOMAS, G. G., 1971: Observations with the scanning electron microscope on the early stages of hop leaf infection by *Pseudoperonospora humuli*. *Physiol. Plant Pathol.* 1, 345—349.
26. — — and — — , 1973: Factors affecting zoospore responses towards stomata in hop downy mildew (*Pseudoperonospora humuli*) including some comparisons with grapevine downy mildew. *Physiol. Plant Pathol.* 3, 405—417.
27. SARGENT, J. A., TOMMERUP, I. C. and INGRAM, D. S., 1973: The penetration of a susceptible lettuce variety by the downy mildew fungus *Bremia lactucae* REGEL. *Physiol. Plant Pathol.* 3, 231—239.
28. SHIMONY, C. and FRIEND, J. 1975: Ultrastructure of the interaction between *Phytophthora infestans* and leaves of two cultivars of potato (*Solanum tuberosum* L.) Orion and Majestic. *New Phytol.* 74, 59—65.
29. — — and — — , 1977: The ultrastructure of the interaction between *Phytophthora infestans* (MONT.) DE BARY and tuber discs of potato (*Solanum tuberosum* L.) cv. King Edward. *Physiol. Plant Pathol.* 11, 243—249.
30. SHIRAIISHI, T., OKU, H., ISONO, M. and OUCHI, S., 1975: The injurious effect of pisatin on the plasma membrane of pea. *Plant Cell Physiol.* 16, 939—942.
31. SKIPP, R. A. and SAMBORSKI, D. J., 1974: The effect of the Sr6 gene for host resistance on histological events during the development of stem rust in near-isogenic wheat lines. *Canad. J. Bot.* 52, 1107—1115.
32. — — , SELBY, C. and BAILEY, J. A., 1977: Toxic effects of phaseollin on plant cells. *Physiol. Plant Pathol.* 10, 221—227.
33. SPURR, A. R., 1969: A low viscosity epoxy resin embedding medium for electron microscopy. *J. Ultrastruct. Res.* 26, 31—43.

Eingegangen am 24. 7. 1980

Dr. P. LANGCAKE  
Shell Biosciences Laboratory  
Sittingbourne Research Centre  
Sittingbourne, Kent ME 9 8 AG  
U.K.